Magnetic interaction between manganese (2+) atoms through aquo bridges and bifurcated cyano groups



2007 J. Phys.: Condens. Matter 19 056202

(http://iopscience.iop.org/0953-8984/19/5/056202)

INSTITUTE OF PHYSICS PUBLISHING JOURNAL OF PHYSICS: CONDENSED MATTER

J. Phys.: Condens. Matter **19** (2007) 056202 (11pp) doi:10.1088/0953-8984/19/5/056202

# Magnetic interaction between manganese (2+) atoms through aquo bridges and bifurcated cyano groups

**R Martínez-García[1], L Reguera[2], M Knobel[3] and E Reguera[1,4,5]**

[1] Institute of Science and Technology of Materials, University of Havana, 10400 Havana, Cuba
[2] Faculty of Chemistry, University of Havana, San Lazaro and L, 10400 Havana, Cuba
[3] Institute of Physics 'Gleb Wataghin', UNICAMP, 13083-970 Campinas SP, Brazil
[4] Center for Applied Science and Advanced Technology of IPN, Mexico, DF, Mexico

E-mail: ereguera@yahoo.com

Received 7 November 2006, in final form 22 December 2006
Published 15 January 2007
Online at stacks.iop.org/JPhysCM/19/056202

**Abstract**

The magnetic interaction between adjacent manganese atoms through aquo double bridges in $Mn_2[M(CN)_6]\cdot xH_2O$ where $x = 8$ and 2 and M = Fe, Ru, Os, was studied. Through these bridges a relatively weak antiferromagnetic interaction is established with an estimated Curie–Weiss temperature, $|\theta_{CW}|$, close to 4 K and a super exchange constant, $|J|$, of 0.27 $cm^{-1}$. When these materials are dehydrated the antiferromagnetic interaction between the Mn atoms undergoes a dramatic increase, with estimated values for $|\theta_{CW}|$ and $|J|$ of 61 K and 4.11 $cm^{-1}$, respectively. Such reinforcement in the magnetic interaction is accompanied by a shift of 32 $cm^{-1}$ for the $\nu$ (CN) vibration towards the low frequency region while for the iron compound the Mössbauer spectrum, initially a single line, becomes a quadrupole splitting doublet of relatively low isomer shift ($\delta$) value. The Curie constant of the involved Mn atoms shows a negative correlation with the observed shifts in $\nu$ (CN) and $\delta$ on dehydration. From the observed magnetic behaviour and the spectroscopic data a double coordination of an N end of the CN ligand to two Mn atoms is proposed. Such strong magnetic interaction through the N atom of the CN ligand could be used as a prototypical bridge to obtain high $T_c$ molecular magnets.

S Supplementary data are available from stacks.iop.org/JPhysCM/19/056202

## 1. Introduction

The magnetic interaction between transition metal ions in cyano complexes, mainly Prussian blue (PB) analogues, has been an active interdisciplinary research area in the last few

[5] Author to whom any correspondence should be addressed.

years [1, 2]. The magnetic interaction is established by the electron cloud of the metals overlapping through the CN bridges. Several PB analogues are included in those molecular magnets with the highest temperature of magnetic ordering ($T_c$) [3–5]. Many unusual effects reported in PB analogue-based molecular magnets, e.g. mixed ferro/ferrimagnetism [6, 7], exhibition of two compensation temperatures [8, 9], photo-induced magnetism [10] and photo-induced magnetic pole reversal [11], among others, are related to the high flexibility that this family of molecular materials offers to combine different metal ions within the same framework. The hexacyanometallate block, $[M(CN)_6]$, has also been used for the bottom-up building of high spin polynuclear molecules [12]. In this paper the magnetic interaction between adjacent manganese (2+) atoms within a non-magnetic matrix of linked hexacyanometallate (II) blocks, $Mn_2[M(CN)_6]\cdot xH_2O$ with M = Fe, Ru, Os, is discussed. In the hydrated form of the studied solids the Mn(2+) atoms remain linked through two aquo bridges, but when these bridges are removed the manganese atoms appear linked by bifurcated N ends of the CN groups. This change of bridge between the manganese atoms leads to a dramatic variation in their magnetic interaction. The magnetic measurements were complemented by data from x-ray diffraction (XRD), thermo-gravimetric analyses and infrared (IR) and Mössbauer spectroscopies. To the best of our knowledge, the magnetic interaction between adjacent Mn(2+) atoms in such a coordination environments has not been previously reported.

## 2. Experimental details

Manganese ferrocyanide was prepared by mixing aqueous solutions (0.01 M) of manganese chloride and ferrocyanic acid ($H_4[Fe(CN)_6]$ prepared *in situ* [13]). The formed precipitate was aged for 2 days within the mother liquor, then separated by filtration and washed several times with distilled water and finally air dried until it had constant weight. Manganese ruthenocyanide and osmocyanide were prepared by the same procedure but from the corresponding potassium hexacyanometallate (II). When manganese ferrocyanide is precipitated from potassium ferrocyanide, the mixed Mn–K salt is obtained. The potassium hexacyanoruthenate (II) and hexacyanoosmate (II) used were prepared from $RuCl_2$ and $OsO_4$ by alkaline fusion with KCN, and then re-crystallized several times. The nature and purity of all the intermediate and end products were tested by IR spectroscopy and XRD measurements. The degree of hydration of the samples was estimated by using thermo-gravimetric (TG) curves.

The TG curves were run under a $N_2$ atmosphere (100 ml $min^{-1}$) using a thermo-balance (TGA 2950 model from TA instruments) operated in the high resolution mode. IR spectra were collected by the KBr pressed disc technique and an FT spectrophotometer (Genesis Series from Atti Matson). The magnetic data were collected at low temperature using a SQUID magnetometer (Quantum Design MPMS-XL7), for the as-synthesized materials and after certain heat treatments at temperatures indicated by the TG results. The heat treatments were carried out *in situ* under vacuum within the magnetometer. The Mössbauer spectra were recorded at room temperature using a constant acceleration spectrometer operated in the transmission mode and a $^{57}Co/Rh$ source. A glass cell with windows transparent to $\gamma$-rays where the sample can be dehydrated *in situ* was used to obtain Mössbauer spectra of the iron complex with different degrees of hydration. The spectra were fitted by a least-squares minimization algorithm and pseudo-Lorentzian line shape in order to obtain the values of isomer shift ($\delta$), quadrupole splitting ($\Delta$) and linewidth ($\Gamma$). The values of $\delta$ are reported relative to sodium nitroprusside. XRD powder patterns were recorded in the Bragg–Brentano geometry using Cu K$\alpha$ radiation and indexed using the program *DicVol* [14].

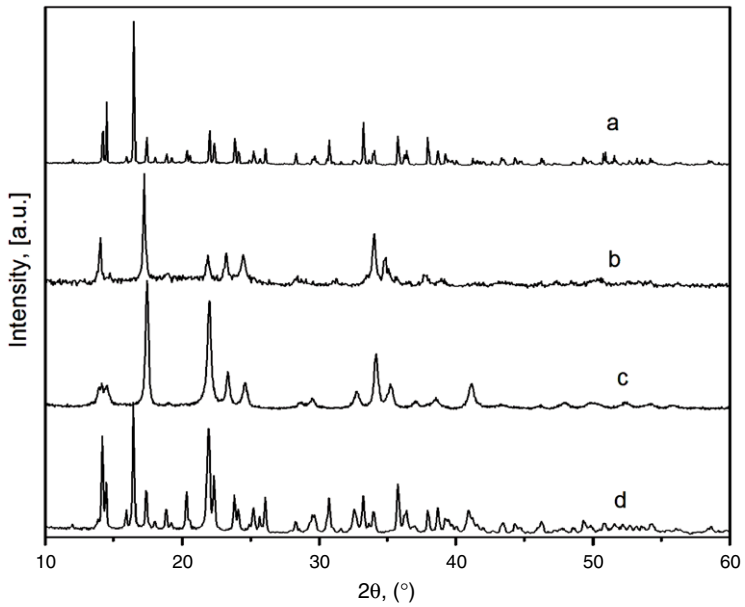


**Figure 1.** XRD powder patterns of (a) $Mn_2[Fe(CN)_6]\cdot 8H_2O$ (space group $P2_1/n$), (b) $Mn_2[Fe(CN)_6]\cdot 2H_2O$, (c) $Mn_2[Fe(CN)_6]$ and (d) $Mn_2[Fe(CN)_6]$ after immersion in water for 3 days (re-hydrated). For comparison, patterns (a) and (b) were recorded using the same counting time per point. Patterns (c) and (d) were recorded with a larger counting time.

## 3. Results and discussion

### *3.1. Nature of the studied solids*

According to the XRD, TG and IR data (figures 1 and 2) the obtained samples correspond to compounds with the following unit formula: $Mn_2[M(CN)_6]\cdot 8H_2O$ with M = Fe(II), Ru(II), Os(II)—from now on $Mn_2M$. These solids crystallize in the monoclinic space group $P2_1/n$, and their crystal structure is known [15, 16]. In the crystal structure two adjacent Mn atoms, at 3.70 Å, related by an inversion centre, are linked by two water molecules, forming a moiety composed of two edge-shared octahedra (figure 3). No direct interaction can take place between the Mn atoms because they remain very distant (3.70 Å). The Mn–$OH_2$ distance is close to 2.40 Å. The inter-atomic distance between the water oxygen atoms is close to 3.20 Å, too large to suppose that these two water molecules are interacting through hydrogen bond bridges. The Mn–O–Mn angle in these moieties remains around 101°. The manganese cluster–cluster distance is above 10 Å; which is the Mn–NC–M–CN–Mn chain length. The coordination sphere of the Mn atom is completed by a third water molecule plus three N atoms from CN groups. The materials also contain zeolitic waters (four per unit formula) sited in interstitial spaces whose existence is mainly due to the –C≡N– bridge length of about 4.5 Å. These zeolitic waters are stabilized within these structural free spaces by hydrogen bonding interactions with the coordinated ones. The interstitial spaces remain in communication to form a trapezoidal channel system of about 3.9 × 4.2 Å.

In the studied solids only the Mn atoms have unpaired electrons, Mn(2+): $t_{2g}^3 e_g^2$ ($S = 5/2$). The M atom remains in a low spin state with six electrons in their $t_{2g}$ orbitals ($S = 0$). The Mössbauer spectrum of the iron complex is a single line with an isomer shift ($\delta$) value typical of low spin Fe(II) (figure 4(a), table 1). From this fact the studied hydrates can be considered as

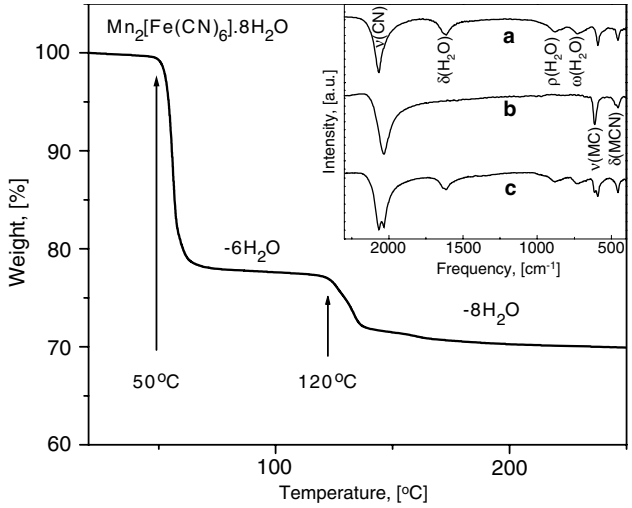


**Figure 2.** Thermo-gravimetric curve for $Mn_2[Fe(CN)_6]\cdot 8H_2O$. The dehydration process takes place in two steps, with formation of an intermediate dihydrate. Inset: the 22 000–400 $cm^{-1}$ region of IR spectra where the vibrations of the studied materials are indicated: (a) $Mn_2[Fe(CN)_6]\cdot 8H_2O$, (b) $Mn_2[Fe(CN)_6]\cdot 0H_2O$, (c) $Mn_2[Fe(CN)_6]\cdot xH_2O$ (partially re-hydrated). When the anhydrous sample is maintained in humid air or immersed in water the aquo bridges are progressively restored (c).

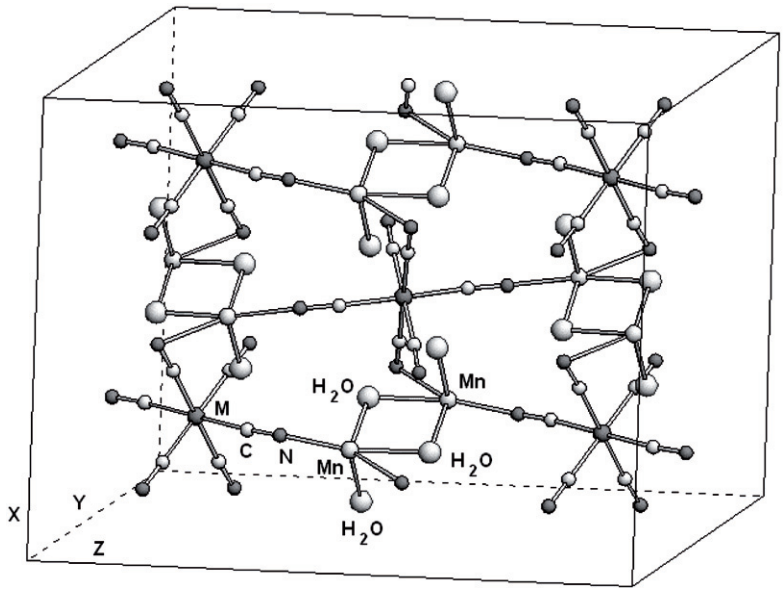


**Figure 3.** Manganese atoms linked by two aquo bridges in the structure of $Mn_2[M(CN)_6]\cdot 8H_2O$ (M = Fe, Ru, Os). This illustration was prepared from the reported crystal data for this family of compounds [15, 16].

small clusters (dimers), $Mn_2(H_2O)_2$, within a non-magnetic matrix and with a weak interaction among them.

A distinctive feature for the studied materials, and also for the cadmium analogues [17], within all the known hexacyanometallates is the appearance of the above mentioned aquo

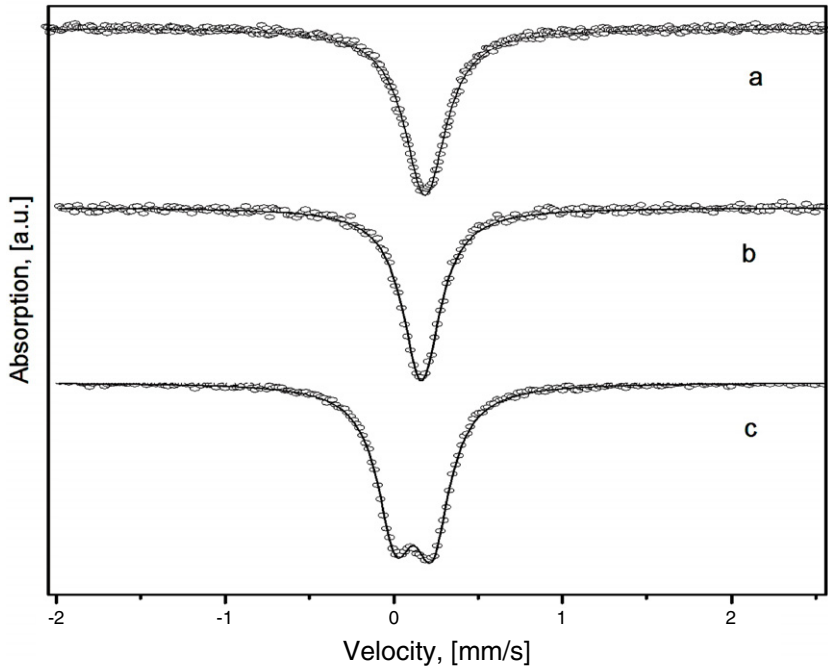


**Figure 4.** Mössbauer spectra at room temperature of (a) $Mn_2[Fe(CN)_6]\cdot 8H_2O$, (b) $Mn_2[Fe(CN)_6]\cdot 2H_2O$ and (c) $Mn_2[Fe(CN)_6]$.

**Table 1.** Magnetic, IR and Mössbauer parameters for the studied materials.

| Sample | $\lvert\theta_{CW}\rvert$ (K) | $C$ ($cm^3$ K $mol^{-1}$) | $\lvert J\rvert$ ($cm^{-1}$) | $\nu$ (CN) ($cm^{-1}$) | $\delta$ [a] (mm $s^{-1}$) | $\Delta$ (mm $s^{-1}$) |
|---|---|---|---|---|---|---|
| $Mn_2Fe$, $x = 8$ | 3.5(2) | 4.18(3) | 0.27 | 2066 | 0.188 | 0.0 |
| $Mn_2Fe$, $x = 2$ | 5.5(1) | 4.16(2) | 0.45 | 2066 | 0.163 | 0.0 |
| $Mn_2Fe$, $x = 0$ | 61.5(3) | 5.35(6) | 4.11 | 2032 | 0.072 | 0.282 |
| $Mn_2Ru$, $x = 8$ | 3.4(2) | 4.54(2) | 0.30 | 2079 | — | — |
| $Mn_2Ru$, $x = 0$ | 53.5(1) | 5.21(8) | 3.71 | 2039 | — | — |
| $Mn_2Os$, $x = 8$ | 3.9(2) | 4.20(2) | 0.36 | 2069 | — | — |
| $Mn_2Os$, $x = 0$ | 48.3(1) | 4.66(6) | 3.29 | 2025 | — | — |

[a] $\delta$ value relative to sodium nitroprusside. The fitting error in $\delta$ and $\Delta$ remains below 0.01 mm $s^{-1}$.

double bridges between two neighbouring metals. Such bridges are identified in the IR spectra by rocking, $\rho(H_2O)$, and wagging, $w(H_2O)$, vibrations of the water molecules involved in them, which are observed in the 820–680 $cm^{-1}$ region (figure 2, inset a). The remaining absorption bands in the IR spectra of the studied materials are those from $\nu$ (OH) and $\delta$ (HOH) vibrations of the crystal water and the ones related to the hexacyanometallate ion, $\nu$ (CN), $\delta$ (MCN) and $\nu$ (MC). The frequencies of these vibrations have been reported [18].

### *3.2. Behaviour of the materials on heating*

Manganese and cadmium hexacyanometallates (II) form two isomorphous series with similar properties in their hydrated state [17]. However, cadmium is a bigger metal with a relatively weak interaction with its coordination water. This favours an easy dehydration of the cadmium analogues to form materials with a relatively high crystalline ordering [17, 19]. The reported

properties for the anhydrous cadmium series help us to understand some features of the studied anhydrous manganese compounds.

The TG curves of the studied samples show two steps of weight loss in the dehydration temperature region (figure 2). From about 50 °C the zeolitic (hydrogen bonded) water molecules and a coordinated one evolve, and a dihydrate results. The hydrogen bonded waters in cyanometallates usually evolve below 60 °C [20]. The water molecule has a kinetic diameter of 2.65 Å [21], sufficiently small to allow its easy diffusion through the porous framework of the material, with a channel cross section of about 3.9 × 4.2 Å. The adsorption enthalpies of zeolitic water molecules in cyanometallates are relatively low, below 10 kJ $mol^{-1}$ [20]. The formed hydrogen bridges are of medium strength. Even the coordinated waters can be removed by relatively soft heating. The coordination site is always the outer metal, in this case the manganese atom, with a relatively low polarizing power [22]. Usually the zeolitic and at least a fraction of coordinated waters in hexacyanometallates evolve through a practically continuous process, without a definite inflection in the TG curve [23]. From about 65 °C the studied material becomes dihydrate (figure 2). The formation of the aquo bridge leads to a high stabilization for the coordinated water. These bridges remain stable up to 120 °C where they are disrupted and the water molecules liberated. From this last temperature (120 °C) the $\rho(H_2O)$ and $w(H_2O)$ IR absorption bands disappear, and also the $\nu$ (OH) and $\delta$ (H–O–H) ones, indicating that all the water abandons the solid (figure 2, inset (b)). No water molecules remain occluded within the solid.

The removal of the zeolitic and of the third coordinated (non-bridged) waters leads to significant structural changes in the studied materials. The XRD powder patterns of samples annealed above 50 °C do not correspond to the $P2_1/n$ space group characteristic of the initial octahydrate (figure 1(b)). In addition, the sample crystalline ordering decreases, as suggested by the broadening of the diffraction peaks. During this first dehydration step the release of zeolitic water leaves a large free space. This fact, together with the loss of a water molecule from the manganese coordination environment, induces the observed structural transformation to form a more compact material. The obtained XRD powder pattern for the formed dihydrate is of poor quality but it can be tentatively indexed as orthorhombic ($\mathbf{a} = 9.89(2)$, $\mathbf{b} = 8.95(1)$; $\mathbf{c} = 9.19(1)$ Å). This is equivalent to a cell volume reduction per unit formula of 9.5% (with $Z = 2$) relatively to the initial octahydrate. The Mössbauer spectrum for the formed dihydrate can be fitted by a single line with an isomer shift slightly lower than the one observed for the initial hydrate (figure 4(b), table 1). The observed decrease for the isomer shift value results from the removal of a ligand (a water molecule) from the environment of the manganese atom. This induces a higher interaction of the metal with the remaining ligands, favouring a higher charge subtraction from the CN ligands, mainly through their $5\sigma$ orbitals. As a charge redistribution effect, the $\pi$-back bonding interaction between the iron atom and the CN group at the C end increases, reducing the availability of 3d electrons on the iron atom and of their shielding effect on the s electron density at the iron nucleus. This explains the observed variation in $\delta$ when the non-bridged coordinated waters are removed. An analogous effect is detected by magnetic measurements (discussed below).

The disruption of the water bridges leads to additional structural changes on the studied material. The XRD powder pattern of the anhydrous sample is typical of a material of low crystalline ordering (figure 1(c)). For the iron complex the pattern can be tentatively indexed as orthorhombic ($\mathbf{a} = 9.71(1)$, $\mathbf{b} = 8.89(1)$; $\mathbf{c} = 6.23(1)$ Å). The estimated cell volume reduction per unit formula is 41% (from $Z = 2$), relative to the initial hydrate. A similar cell reduction per unit formula was calculated from the reported crystal structure for the cadmium–iron analogue [17, 19]. The removal of crystal water leads to the formation of a more compact material. All the attempts to refine the crystal structure for the anhydrous

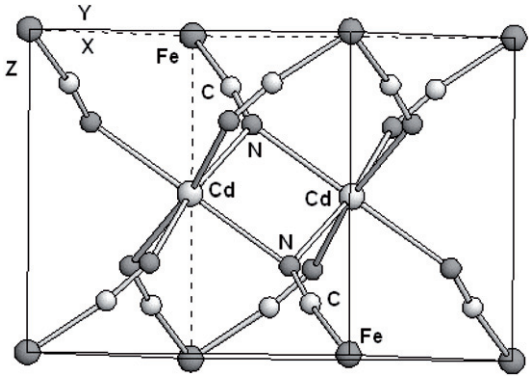


**Figure 5.** Coordination environment for the cadmium atom in anhydrous $Cd_2[Fe(CN)_6]$ ($P\bar{3}1m$). The same N end of the CN ligand is coordinating with two cadmium atoms. This illustration was prepared from the reported crystal data for this compound [19]. The manganese and cadmium analogues are isomorphous in their hydrated forms. All the experimental evidence suggests that in the anhydrous forms the Mn atoms are also bridged by bifurcated N ends.

phase were unsuccessful; poor figures of merit were always obtained for the refinement processes. Such structural transformation is accompanied by two other pieces of additional spectroscopic evidence: a shift towards the low frequency region for the $\nu$ (CN) vibration of about 32 $cm^{-1}$ (figure 2, inset (b)), and a change in the Mössbauer spectrum for the iron complex (figure 4(c), table 1). The Mössbauer spectrum of this composition, which is initially a single line, appears in the anhydrous phase as a resolved doublet with a quadrupole splitting ($\Delta$) value of 0.282 mm $s^{-1}$ and a particularly low value of $\delta$, 0.072 mm $s^{-1}$. This low value of $\delta$ was interpreted as a stronger interaction of the Mn atoms with the CN ligand at the N end, inducing a large charge subtraction via $\pi$-back bonding from the iron atom. Such charge subtraction must be anisotropic because an electric field gradient around the iron nucleus is sensed. The other experimental evidence, the $\nu$ (CN) frequency shift, could also be explained, at least partially, by the induced $\pi$-back donation from the inner metal, which weakens the C≡N triple bond.

The loss of all the crystal water leaves the Mn atom with only three ligands in the coordination sphere. This is an unstable configuration. However, the anhydrous phase shows a certain stability even in a humid environment. The anhydrous phase remains stable at room conditions without special precautions. It seems that the structural transformation related to the disruption of the aquo bridges and the water evolution is accompanied by a higher coordination for the Mn atom. The option is the bond of the N end to two Mn atoms. No other ligand is available in the studied anhydrous solids. This is equivalent to replacing the aquo bridges by 'N' bridges. This could explain the observed changes in the IR and Mössbauer spectra upon sample dehydration, and the relatively high stability observed for the metastable anhydrous phase. Such behaviour supposes a change in the CN group electronic configuration to enable the coordination of the N end to two Mn atoms (a bifurcated N end). This coordination for the CN group is rare in transition metal cyano complexes but is mentioned as possible in [24] and is reported for the cadmium and iron analogue in [19]. According to the reported crystal structure for anhydrous $Cd_2Fe$, an N end serves as a ligand for two metals (figure 5). The above discussed changes in IR and Mössbauer spectra for $Mn_2M$ on dehydration have also been observed for $Cd_2M$ analogues [17]. This is consistent with the above proposed coordination mode for the manganese atom in anhydrous $Mn_2M$ phases.

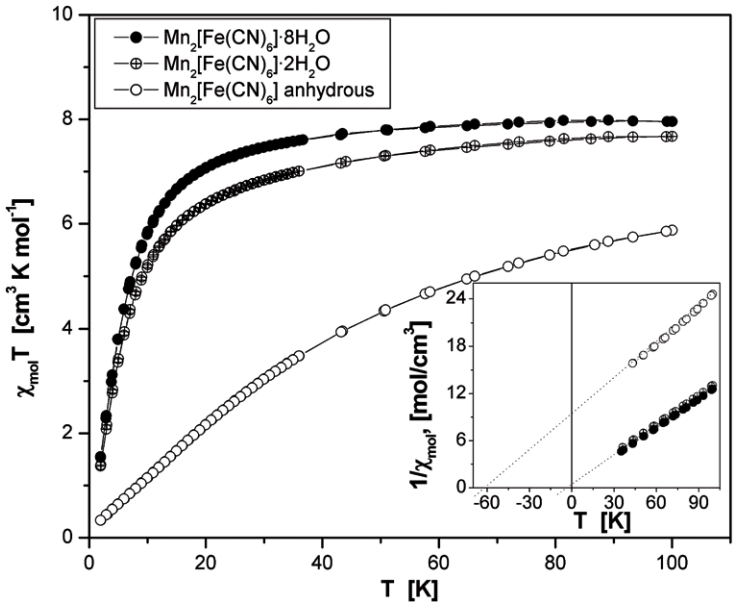


**Figure 6.** Temperature dependence of $\chi_{\mathrm{mol}}T$ for the hydrated and anhydrous Mn(II) ferrocyanide. Inset: temperature dependence of the inverse magnetic susceptibility.

When anhydrous $Mn_2M$ samples are immersed in water or maintained for several days in a humid environment a progressive re-hydration process is detected. The simplest test is their IR spectra where the $\rho(H_2O)$ and $w(H_2O)$ absorption bands reappear (figure 2, inset (c)). The XRD powder pattern (figure 1(d)) is conclusive on the reversibility of the dehydration process, although in the re-hydrated sample certain structural disorder persists.

### *3.3. Magnetic interaction between manganese atoms*

Figure 6 shows the temperature dependence of the molar magnetic susceptibility per temperature ($\chi_{\mathrm{mol}}T$) for hydrated $Mn_2Fe$. Similar curves were obtained for the analogues of Ru and Os (see supplementary information available at stacks.iop.org/JPhysCM/19/056202). The value of $\chi_{\mathrm{mol}}T$ versus $T$ gradually decreases, indicating a weak antiferromagnetic interaction, which becomes evident below 40 K. From the fitting of the Curie–Weiss law, $\chi^{-1} = (T - \theta_{\mathrm{CW}})/C$, for the paramagnetic region of the $1/\chi_{\mathrm{mol}}$ versus $T$ curve (figure 6, inset), the value for the Curie–Weiss constant, $\theta_{\mathrm{CW}}$, was estimated. The negative $\theta_{\mathrm{CW}}$ value (table 1) corresponds to an antiferromagnetic interaction between the two Mn atoms, as expected. The aquo bridges are formed through the free pair of $sp^3$ orbitals of the water molecule. These orbitals are involved in $\sigma$-donor bonds with the Mn atoms. These bonds have a relatively low participation from the metal electrons and from this fact the electron cloud of the metals overlapping through the water molecules is very low. An additional factor to be considered is the Mn–$(H_2O)_2$–Mn bond angle, which is 101°. A non-linear coordination bond does not favour a strong super-exchange interaction between the metal centres [25]. These features explain the relatively small values obtained for $|\theta_{\mathrm{CW}}|$ in the studied hydrates, which are in the range of 3–4 K (table 1). An analogous weak antiferromagnetic interaction has been reported to occur in Mn(2+) atoms through a simple aquo bridge, Mn–$(H_2O)$–Mn [26]. This suggests that the non-linear coordination bond in the $Mn_2(H_2O)_2$ moiety could have a minor effect on the observed weak antiferromagnetic interaction.

As mentioned above, the studied hydrates can be considered as $Mn_2(H_2O)_2$ dimers regularly dissolved within a non-magnetic matrix and with a weak interaction among them. These are appropriate conditions to fit the experimental magnetic data according to an isotropic exchange coupling model in order to infer the values of the exchange coupling constant $|J|$ and of the Curie constants for the metals involved. In such a model the exchange constant $J$ and the molecular field parameter $W$ are related according to [27]

$$W = \frac{z\,|J|}{N_A g^2 \mu_B^2}; \tag{1}$$

where $z$ is the number of magnetic nearest neighbours, $N_A$ is Avogadro's constant, $g$ is a mean Landé factor and $\mu_B$ is the Bohr magneton. In turn, from the Néel theory for the molecular field [28], the value of $W$ can be calculated from the experimental molar susceptibility data by the following expression:

$$\frac{1}{\chi_{mol}} = \frac{T^2 - W^2 C_A C_B}{(C_A + C_B)T - 2W C_A C_B}; \tag{2}$$

where $A$ and $B$ are the magnetic nearest neighbours (in our case the Mn atoms) and $C_A$ and $C_B$ are their Curie constants. Since the involved metals are identical, then, $C_A = C_B = C$.

The non-linear fitting of all the $\chi_{mol}$ versus $T$ data according to equation (2) or to the related $\chi_{mol}T$ dependence provides the best values for the parameters $W$ and $C$. Figure 6 shows the experimental $\chi_{mol}T$ versus $T$ curve for $Mn_2Fe$ and the corresponding non-linear fitting. The obtained values for $W$ and $C_{Mn}$ are 4.18(3) $cm^3\ mol^{-1}$ K and 0.95(3) $cm^{-3}$ mol, respectively. The value for the exchange parameter $|J|$ was then calculated using the equation (1) resulting in $|J| = 0.27\ cm^{-1}$. This relatively small absolute value for $J$ agrees with the estimated Curie–Weiss constant ($|\theta_{CW}| = 3.5$ K) and also with the nature of the bridging group between the Mn atoms, i.e. the water molecule, which has a low ability to allow a significant overlap of the metallic electron cloud. This procedure to derive the absolute value for $J$ and for the Curie constant ($C$) has been frequently used in the study of molecular magnets based on PB analogues [29].

When the $Mn_2M$ samples are dehydrated at 60 °C, the $\chi_{mol}T$ versus $T$ curve preserves its appearance, with practically the same paramagnetic region but with an appreciable increase in the absolute values for $\theta_{CW}$ and $J$ (see figure 6 and table 1). This agrees with the behaviour observed from TG and IR data. At this dehydration step two coordinated waters per unit formula and all the zeolitic ones evolve and only the aquo bridges remain. In these conditions the resulting pentacoordinated Mn atoms continue to interact through the two water molecules. However, the removal of the third coordinated water from the Mn atom environment induces a reinforcement of the metal interaction with the bridged waters and through them with the neighbouring metal. This explains the observed increase in $|\theta_{CW}|$ and $|J|$.

The sample heating at a temperature of 120 °C or higher leads to a dramatic enhancement of the magnetic interaction between the Mn atoms (figure 6). This corresponds to a large increase in the overlapping of the metallic electron cloud. Such behaviour supports the above proposed structural model, where neighbouring manganese atoms remain bridged by bifurcated N ends of CN groups. The magnetic ordering in PB analogues is related to the ability of the CN group to delocalize charge from the inner metal via $\pi^*$-back donation and place it on the N end. The super-exchange interaction in PB analogue-based magnets takes place through such delocalized charge. In anhydrous $Mn_2M$ such a role may be played by the bifurcated N end. For the Mn–N–Mn bond significant participation of the electrons from the involved metals is expected in order to explain the observed strong antiferromagnetic interactions between them. The estimated absolute values for $\theta_{CW}$ and $J$ for anhydrous $Mn_2M$ samples are collected in table 1. The variation in the value of $|\theta_{CW}|$ on the removal of the aquo bridges, from 3.5

to 61.5 for $Mn_2Fe$, represents an increase of 18 times, and of 15 times for $|J|$, from 0.27 to 4.11 $cm^{-1}$. Such variations in the absolute values for $\theta_{CW}$ and $J$ could be related to the following two factors: (a) a shorter Mn–Mn distance related to a stronger covalent ligand–metal bond inducing a higher metal charge delocalization on the ligand; (b) a more favourable metal–ligand–metal angle which favours a higher overlapping of metal orbitals. It seems that the observed change in $\theta_{CW}$ and $J$ results from a combination of both factors, as suggested by a comparison of the reported crystal structures for the $Cd_2Fe$ analogue in its hydrated and anhydrous forms [17, 19]. In $Cd_2[Fe(CN)_6]\cdot 8H_2O$ the Cd–$L_2$–Cd angle is 101°, while in $Cd_2[Fe(CN)_6]$ it is 98.5° [17, 19]. The reduction in the Cd–L distance is significantly higher, of about 0.1 Å (2.53 versus 2.42 Å).

The obtained values for the Curie constant ($C$) in hydrated and anhydrous $Mn_2M$ samples are collected in table 1. Neglecting the effect of second nearest neighbours [25], the Curie constant for both hydrated and anhydrous forms of the studied materials must be very similar. At sufficiently high temperatures the asymptotic value for the $\chi_{mol}T$ dependence derived from equation (2) results in $C_A + C_B$, where the antiferromagnetic interaction between the metal centres is minimized. However, on the removal of the aquo bridges the value of $C$ increases. This corresponds to an inverse correlation with the observed variation for $\nu$ (CN) and $\delta$ (table 1). That behaviour for the value of $C$ could be attributed to a higher covalence of the metal–ligand bond for the anhydrous phase—an expected effect according to the Mössbauer spectroscopy results. Such a higher covalence on the removal of water leads to an increase in the charge subtraction from the iron atom, via $\pi$-back donation, and its delocalization on the manganese atom, and probably to the observed variation in the Curie constant.

## 4. Conclusions

In the studied $Mn_2M$ hydrates the antiferromagnetic interaction between the Mn atoms through the aquo bridges is particularly weak, which was attributed to the bonding properties of the water molecule, particularly to its low ability to allow a significant contribution from the metallic electron cloud to the coordination bond. When the water bridges are removed a structural transformation takes place and the Mn atoms become bridged through bifurcated N ends. The bond formed between the metal and the CN group at the N end shows an increased covalence as detected by the stronger antiferromagnetic interaction between adjacent Mn atoms, but also by the IR and Mössbauer data. The observed changes for the Curie constant, the Curie–Weiss temperature and the exchange parameter $J$ on the removal of water support a higher delocalization of metal charge through the N end of the CN group for the anhydrous phase. In those PB analogue-based molecular magnets where such double bridges through the N end of the CN group could be implemented, relatively high $T_c$ values could be expected due to a higher density of metal centres but also because of a highly covalent metal–ligand bond.

## Acknowledgments

RMG acknowledges the support provided by the CLAF-ICTP program for his PhD studies. ER is grateful for the support provided by CLAF-ICTP for carrying out research activities on molecular materials. The authors thank C Vazquez-Ramos from IIM-UNAM for TG data acquisition. The support from FAPESP and CNPq (Brazilian agencies) is acknowledged.

## References

[1] Verdaguer M, Bleuzen A, Marvaud V, Vaissermann J, Seuleiman M, Desplanches C, Scuiller A, Train C, Garde R, Gelly G, Lomenech C, Rosenman I, Veillet P, Cartier C and Villain F 1999 *Coord. Chem. Rev.* **190–192** 1023

[2] Dujardin E and Mann S 2004 *Adv. Mater.* **16** 1125
[3] Ferlay S, Mallah T, Ouahes R, Veillet P and Verdaguer M 1995 *Nature* **378** 701
[4] Holmes S M and Girolami G S 1999 *J. Am. Chem. Soc.* **121** 5593
[5] Sato O, Iyoda T, Fujishima A and Hashimoto K 1996 *Science* **272** 704
[6] Ohkoshi S, Iyoda T, Fujishima A and Hashimoto K 1997 *Phys. Rev.* B **56** 11642
[7] Ohkoshi S, Sato O, Iyoda T, Fujishima A and Hashimoto K 1997 *Inorg. Chem.* **36** 268
[8] Ohkoshi S, Abe Y, Fujishima A and Hashimoto K 1999 *Phys. Rev. Lett.* **82** 1285
[9] Ohkoshi S, Hozumi T, Utsunomiya M, Abe Y and Hashimoto K 2003 *Physica* B **329–333** 691
[10] Hatlevik O, Buschaman W E, Zhang J, Manson J L and Millar J S 1999 *Adv. Mater.* **11** 914
[11] Ohkoshi S, Yorozu S, Sato O, Iyoda T, Fujishima A and Hashimoto K 1997 *Appl. Phys. Lett.* **70** 1040
[12] Marvaud V, Decroix C, Scuiller A, Guyard-Duhayon C, Vaissermann J, Gonnet F and Verdaguer M 2003 *Chem. Eur. J.* **9** 1677
[13] Brauer G 1965 *Handbook of Preparative Inorganic Chemistry* 2nd edn, vol 2 (New York: Academic) p 1373
[14] Louer D and Vargas R 1982 *J. Appl. Crystallogr.* **15** 542
[15] Rueg M, Ludi A and Rieder K 1971 *Inorg. Chem.* **10** 1775
[16] Gómez A, Lara V, Bosch P and Reguera E 2002 *Powder Diffract.* **17** 148
[17] Gómez A and Reguera E 2001 *Int. J. Inorg. Mater* **3** 1045
[18] Reguera E, Gómez A, Balmaseda J, Contreras G and Escamilla A 2001 *Struct. Chem.* **12** 59
[19] Gomez A 2002 *PhD Thesis* University of Havana
[20] Balmaseda J, Reguera E, Gómez A, Roque J, Vazquez C and Autie M 2003 *J. Phys. Chem.* B **107** 11360
[21] Sing S W, Everett D H, Haul R A W, Moscou L, Pierotti R A, Rouquerol J and Siemienswska T 1985 *Pure Appl. Chem.* **57** 603
[22] Zhang Y 1982 *Inorg. Chem.* **21** 3886
[23] Martinez-Garcia R, Knobel M and Reguera E 2006 *J. Phys. Chem.* B **110** 7296
[24] Dunbar K R and Heintz R A 1997 *Prog. Inorg. Chem.* **45** 283
[25] Kahn O 1985 *Angew. Chem. Int. Edn Engl.* **24** 834
[26] Goodwin J C, Price D J and Hearth S L 2004 *Dalton Trans.* **18** 2833
[27] Herpin A 1998 *Théorie du Magnétisme (INSTN-PUF, Saclay, France)*
[28] Néel L 1948 *Ann. Phys. Fr.* **3** 137
[29] Ferlay S, Mallah T, Ouahes R, Veillet P and Verdaguer M 1999 *Inorg. Chem.* **38** 229